Optimal Allocation of Dispersed Energy Storage Systems in Active Distribution Networks for Energy Balance and Grid Support

Mostafa Nick, *Student Member, IEEE*, Rachid Cherkaoui, *Senior Member, IEEE*, and Mario Paolone, *Senior Member, IEEE*

***Abstract*—Dispersed storage systems (DSSs) can represent an important near-term solution for supporting the operation and control of active distribution networks (ADNs). Indeed, they have the capability to support ADNs by providing ancillary services in addition to energy balance capabilities. Within this context, this paper focuses on the optimal allocation of DSSs in ADNs by defining a multi-objective optimization problem aiming at finding the optimal trade-off between technical and economical goals. In particular, the proposed procedure accounts for: 1) network voltage deviations; 2) feeders/lines congestions; 3) network losses; 4) cost of supplying loads (from external grid or local producers) together with the cost of DSS investment/maintenance; 5) load curtailment; and 6) stochasticity of loads and renewables productions. The DSSs are suitably modeled to consider their ability to support the network by both active and reactive powers. A convex formulation of ac optimal power flow problem is used to define a mixed integer second-order cone programming problem to optimally site and size the DSSs in the network. A test case referring to IEEE 34 bus distribution test feeder is used to demonstrate and discuss the effectiveness of the proposed methodology.**

***Index Terms*—Ancillary services, energy storage, mixed integer second order cone programming, power distribution, power system planning.**

NOMENCLATURE:

DSS	Dispersed storage system.
DG	Distributed generation.

Variables:[1]

u_i^{DSS}	Binary variable associated with the presence of energy storage at bus i.
$u_{i,y,Sc,t}^{\mathrm{DG}}$	Binary variable associated with the on/off states of a given DG unit.
S_i^{DSS}	Power rating of a given DSS at bus i.
E_i^{DSS}	Energy reservoir of a given DSS at bus i.
$V_{i,y,Sc,t}$	RMS value of bus i voltage at time t, scenario Sc, and year y.
$F_{(l)ij,y,Sc,t}$	Current flow of the generic line (l) between buses i and j at time t, scenario Sc, and year y.
$v_{i,y,Sc,t}$	Square of voltage at bus i at time t, scenario Sc, and year y.
$f_{(l)ij,y,Sc,t}$	Square of current flow of the generic line (l) between buses i and j at time t, scenario Sc, and year y.
$P_{ij,y,Sc,t}Q_{ij,y,Sc,t}$	Active/reactive line power flows between buses i and j at time t, scenario Sc, and year y.
$P_{i(j),y,Sc,t}^{\mathrm{DSS}}Q_{i(j),y,Sc,t}^{\mathrm{DSS}}$	Active/reactive power production /consumption of a given DSS unit connected to bus $i(j)$ at time t, scenario Sc, and year y
$P_{i(j),y,Sc,t}^{\mathrm{DG}}Q_{i(j),y,Sc,t}^{\mathrm{DG}}$	Active/reactive power production of a given DG unit connected to bus $i(j)$ at time t, scenario Sc, and year y
$P_{j,y,Sc,t}^{\mathrm{Cur}}$	Active load curtailed on the bus i at time t, scenario Sc, and year y
$Q_{ij,y,Sc,t}^{\mathrm{sh}}$	Reactive power associated with shunt susceptance of the line between buses i and j at time t, scenario Sc, and year y.
$loss_{i,y,Sc,t}^{\mathrm{DSS}}$	Resistive losses of DSS i at time t, scenario Sc, and year y.

Manuscript received July 12, 2013; revised November 04, 2013; accepted December 22, 2013. Date of publication February 10, 2014; date of current version August 15, 2014. This work was supported by the project between the EOS Holding and the EPFL Distributed Electrical Systems Laboratory entitled "Advanced control, of distribution networks with the integration of dispersed energy storagesystems". Paper no. TPWRS-00905-2013.

The authors are with the Distributed Electrical Systems Laboratory, École Polytecnique Fédérale de Lausanne (EPFL), Lausanne, Switzerland (e-mail: mostafa.nick@epfl.ch; rachid.cherkaoui@epfl.ch; mario.paolone@epfl.ch).

Color versions of one or more of the figures in this paper are available online at http://ieeexplore.ieee.org.

Digital Object Identifier 10.1109/TPWRS.2014.2302020

[1]All of the parameters and variables are in p.u..

$Aux^V_{i,y,Sc,t}$	Auxiliary variables associated with the linearization of voltage deviation minimization in the objective function.
$Aux^F_{ij,y,Sc,t}$	Auxiliary variables associated with the linearization of current flow minimization in the objective function.
$C^E_{y,Sc,t}$	Energy cost from upper grid at time t, scenario Sc, and year y.
CF^{DG}_i	Cost function of a given DG unit at bus i.

Parameters:

FC_i	Capital installation cost of a given DSS at bus i (\$).
$InvC^P_i$	Investment cost related to the power rating of a given DSS at bus i (\$/kW).
$InvC^E_i$	Investment cost related to the reservoir capacity of a given DSS at bus i (\$/kWh).
α	Annual interest rate.
MC^y_i	Maintenance cost of a given DSS at bus i in year y (\$/kWh/year).
U_{DSS}	Maximum number of buses where DSS units can be installed.
$S^{\mathrm{DSS,max}}_i S^{\mathrm{DSS,min}}_i$	Maximum/minimum power rating of a given DSS unit that can be connected to bus i.[2]
$E^{\mathrm{DSS,max}}_i E^{\mathrm{DSS,min}}_i$	Maximum/minimum energy reservoir capacity of a given DSS unit that can be connected to bus i.
$RU^{\mathrm{DSS}}_i RD^{\mathrm{DSS}}_i$	Ramp-up and ramp-down rates of the DSS at bus i.
$S^T_{\max}$	Total maximum power rating of the DSSs that can be installed in the whole network.
$E^T_{\max}$	Total maximum energy reservoir of the DSSs that can be installed in the whole network.
r^{DSS}_i	Loss factor (resistive) of a given DSS at bus i.
r_{ij}, r_l	Longitudinal resistance of the line between buses i and j (line l)
x_{ij}, x_l	Longitudinal reactance of the line between buses i and j (line l).
$P^D_{j,y,Sc,t} Q^D_{j,y,Sc,t}$	Active/reactive power demand on bus i at time t, scenario Sc, and year y.
$v^{\max}, v^{\min}$	Maximum/minimum limits of the square of the voltage on the network buses.
b^{sh}_j	Total susceptance of the lines connected to bus j.
$P^{\max}_{DG_i}, P^{\min}_{\mathrm{DG}_i} Q^{\max}_{\mathrm{DG}_i}, Q^{\min}_{\mathrm{DG}_i}$	Maximum/minimum active/reactive power production limits of a given DG unit connected to bus i.
$f^{\max}_{ij}$	Maximum current flow rating of line between the busses i and j
$E^{\mathrm{DSS}}_{i,t'=0}$	Initial energy stored in DSS i.
$E^{\min}_{\mathrm{DSS,i}}$	Minimum amount of energy that the DSS energy level can't be less than it.
$W_{\mathrm{vol}} W_{\mathrm{flow}} W_{EP} W_{\mathrm{loss}_{\mathrm{DSS}}}$	Weighting coefficient of the terms composing the objective function.
$V^{\max}_{\mathrm{thr}} V^{\min}_{\mathrm{thr}}$	Maximum and minimum voltage thresholds beyond which voltage deviation will be minimized.
F_{thr}	Maximum feeder current threshold beyond which current feeder flow will be minimized.
Prob_{Sc}	Probability of scenario Sc.

Indices:

i, j	Index of buses.
Sc	Index of scenarios.
t	Index of time interval in each day.
y	Index of the years.
$l, and\ ij$	Index of lines.

[2]In the proposed approach, it has inherently been assumed that the DG and DSS units connected to a given bus are aggregated. Therefore, power and energy quantities refer to the aggregated values.

I. Introduction

As is known, recent research and development associated with the electricity infrastructure are driven by the fast evolution of electrical distribution systems from passive to active ones. Active distribution networks (ADNs) are defined as distribution systems in which embedded generation is actively controlled by suitably defined energy management system (EMS) in order to achieve specific operational objectives (e.g., [1] and [2]). However, the lack of direct controllability of the distributed generation (DG) supplying ADNs represents a major obstacle to the increase of the penetration of DG and, more specifically, of renewable energy resources characterized by a non-negligible volatility.

A typical approach allowing EMSs to optimally control ADNs relies on the direct control of the DG (e.g., [3]). However, it requires large investments in reliable and secure

telecommunication infrastructures. In this respect, a different approach that potentially allows postponing the investment associated to the deployment of the above-mentioned telecommunication infrastructures is the use of Dispersed Storage Systems (DSSs) (e.g., [4], [5]). Indeed, DSSs can provide several services to distribution network operators (DNOs) ranging from local energy balance to ancillary services [6]. In particular, they can be used for: peak shaving and renewable energy compensation [7], [8], network services like voltage and frequency control supports [9], [10]. DSSs are also capable of indirectly control line congestions and, as a consequence, can be used for loss minimization and postpone major network upgrades. It is also worth mentioning that, even if the control of DSSs from the DNO will involve the deployment of a dedicated telecommunication infrastructure, it will be limited to few number of DSS units.

In this context, the first problem associated with the use of DSSs is to optimally allocate them in terms of location and energy/power ratings.

The subject of DG siting and sizing have been largely addressed in the literature (e.g., [11]–[14]). In particular, optimal siting and sizing of DGs with the goal of minimizing network losses has been addressed in [11]. In [12], the problem of optimal DG placement is investigated within the specific context of deregulated electricity markets with the aim of maximizing the social welfare and profits of DG owners. A multi-objective approach taking into account investment and maintenance of DG together with network operation, losses, and capacity adequacy costs is used in [13] and [14] for the optimal siting and sizing of DGs.

The literature related to DSSs optimal siting and sizing has treated the following aspects: in [15] a methodology for sizing energy storage devices within the context of microgrids is presented. The authors used a genetic algorithm (GA) to find the optimal capacities of energy storage with an objective function formulated to minimize the operation costs of the targeted microgrid. In [16], a methodology for allocating energy storage systems in a medium-voltage distribution network is proposed with the aim of decreasing wind energy curtailment and minimizing annual cost of the electricity. The authors in [17] used a hybrid GA, combined with a sequential quadratic programming algorithm to size and site DGs, energy storage, and reactive power compensation systems. The objective function proposed in [17] accounts for the network losses and the costs associated to the network upgrades together with energy flow from the external grid. A hybrid method of dynamic programming with GA has been presented in [18] for the optimal integration of energy storage in distribution networks. The objective was to find the best siting, rating, and control strategy of storage systems, in order to minimize the overall investments and network costs (network upgrade and Joule losses). In [19], the problem of the calculation of the total reserve provided by storage systems of a noninterconnected power network, with large penetration of renewables, is formulated. The peculiarity of the proposed approach consists in the use of the discrete Fourier transform (DFT) to determine the required balancing power in different time-spans. For each time-span (i.e., intra-day, intra-hour, and real-time), the proposed approach identifies, by using the DFT components, the total amount of power/energy required by energy storage systems.

A common drawback of the above-listed works is that they did not account for the capability of DSSs to provide ancillary services to ADNs with particular reference to voltage control and feeders/lines congestion management.

In [4], a preliminary study has been presented in which a specific algorithm for the optimal siting of DSSs to maximize their contribution to voltage control was proposed. Voltage sensitivity coefficients, as a function of the nodal power injections, were used to infer a linear formulation of the problem [20]. The study was performed considering different scenarios associated to DG composed of volatile energy resources (essentially PV-injections). In [21], the optimal siting and sizing of DSSs in ADNs has been addressed with the objective of minimizing the ADN voltage deviations, losses and energy cost imported from the external subtransmission grid. In this respect, a hybrid GA and nonlinear programming approach was used to solve the mixed-integer nonconvex nonlinear problem. However, the approach proposed in [21] is computationally expensive and the global optimal solution is not guaranteed for both fitness function (represented by an optimal ac power flow) and the GA procedure.

Another drawback in the literature is related to the proper treatment of the nonlinearity and nonconvexity of the problem. The above-mentioned papers either use nonconvex formulation of the OPF problem or only address the economic aspects without considering the technical constraints of the networks (e.g., network power flows and bus voltage constraints). Recently, several works have been presented in order to convert the AC-OPF problem into a convex one for networks characterized by a generic topology (e.g., [22]).

With reference to the specific case of radial distribution networks, some relaxations have been proposed in order to make the AC-OPF problem convex. A relaxation of the local load/generation balance is proposed in [23], and it is proven to result into a convex problem. In [24], a sufficient condition is proposed for verification of the relaxed OPF problem exactness. The authors of [21] suggested a relaxation with more conservative constraints for the network nodal voltage limits. A mixed-integer quadratically constrained quadratic programming model is proposed in [25] for the optimal reconfiguration of passive distribution systems.

In this paper we adapted the second-order cone programming (SOCP) OPF approach of [25] to formulate the problem of the optimal allocation of DSSs in ADNs accounting for the presence of dispatchable and nondispatchable DGs. The reactive power associated with shunt impedances of the lines is also added to the model. The DSSs are accurately modeled in terms of active and reactive power capability limits, internal losses and state-of-charge (SoC). Dispatchable DG units are also modeled and added to the problem. In particular, it is assumed that dispatchable DGs have the capability of supporting the network with both active and reactive power like DSSs. Like in [21], the allocation problem is represented by a multi-objective function that, in addition to voltage and loss minimization, is augmented

in this paper. We have accounted for the following elements: 1) augmentation of the objective function in order to include the following fundamental elements not accounted in [21]: minimization of line current flows and load curtailment, minimization of dispatchable DG units operation cost, and maximization of DSS round-trip efficiency; 2) linearization of the objective function; 3) convexification of the problem in order to enable its fast/accurate solution; and 4) account for multiple scenarios generated by a suitable data clustering method.

The remainder of this paper is organized as follows. Section II describes the proposed approach by providing first a brief description of SOCP problems, and then it defines the allocation problem and its optimal solution. Section III illustrates the application example with reference to realistic data and a standard network configuration.Section IV concludes the paper with final remarks concerning the applicability of the proposed procedure.

II. Proposed Approach

A. Second-Order Cone Programming (SOCP)

SOCP problems are nonlinear convex ones where a linear objective function is minimized over the intersection of an affine linear manifold and the product of second order cones (quadratic) (e.g., [26] and [27]). This problem can be solved by efficient primal-dual interior point methods. It is worth noting that several classes of convex optimization problems like, for instance, linear program (LP), quadratic program (QP), and quadratically constrained quadratic program (QCQP), are special cases of SOCP. However, SOCP problems are less general than semidefinite (SDP) ones [26]. Wide varieties of engineering problems can be formulated as SOCP such as filter design, truss design, and so on [26], [27]. In this paper, we propose a mixed-integer SOCP formulation of the optimal DSSs siting and sizing in ADNs. In Section II-B, the developed model is described in detail.

B. Problem Definition

As mentioned in the introduction, the context refers to ADNs with the presence of both dispatchable and nondispatchable generation together with DSSs. It is supposed that the ADN is connected to an external subtransmission grid characterized by a given day-ahead hourly cost of the energy exchange known for a time window of 24 h. The goal is to optimally site and size DSSs in the given radial ADN. The objective function includes two parts: 1) the investment and maintenance costs of DSSs as shown in

$$\mathrm{Obj}_{\mathrm{inv}} = \sum_i ((u_i^{\mathrm{DSS}}\mathrm{FC}_i) + (S_i^{\mathrm{DSS}}\mathrm{Inv}C_i^P) + (E_i^{\mathrm{DSS}}\mathrm{Inv}C_i^E)) + \frac{1}{(1+\alpha)^{(y-1)}}\sum_y\sum_i(\mathrm{MC}_i^y). \quad (1)$$

and 2) operation cost of the grid during the DSSs lifetime (brought to the year of investment).

The cost in (1) is composed of a fixed investment cost for each DSS and the cost related to its relevant power and energy capacities. The maintenance cost (brought to the year of the investment) is also accounted.

The operation objective aims at minimizing a virtual cost associated to the system operation conditions. This virtual cost includes: 1) voltage deviation; 2) feeder current flows; 3) total network losses; 4) cost of energy from the external grid and DGs (including DGs start-up cost); 5) DSSs losses; and 6) load curtailment. Each term in the objective function of operation procedure has a suitable weighting coefficient. The virtual cost is minimized for the whole simulated time period that considers all of the scenarios (Sc), all of the hours (t) in each day, and all of the years (y). The operation objective function is formulated as in (2), shown at the bottom of the page.

The weighting coefficients of each term of (2) have been determined by using the analytic hierarchy process (AHP) proposed by Satty in [28].

In the AHP method, first, a pairwise comparison is done between the objectives. The decision-maker (i.e., the DNO) will define the importance of the each factor in the comparison with all the other factors [28]. It depends on the needs of the decision maker and it can vary from network to network and operator to operator. Then a matrix is built based on these pairwise comparisons and the final weights are calculated based on this metric.

C. Constraints

The constraints of the problem are given as follows.

1) DSSs Installation Constraints:

$$\sum_i u_i^{\mathrm{DSS}} \le U_{\mathrm{DSS}} \quad (3)$$

$$u_i^{\mathrm{DSS}} S_i^{\mathrm{DSS,min}} \le S_i^{DSS} \le u_i^{\mathrm{DSS}} S_i^{\mathrm{DSS,max}} \quad (4)$$

$$u_i^{\mathrm{DSS}} E_i^{DSS,\mathrm{min}} \le E_i^{\mathrm{DSS}} \le u_i^{\mathrm{DSS}} E_i^{DSS,\mathrm{max}} \quad (5)$$

$$\begin{aligned} Obj_{op} = \frac{\mathrm{Prob}_{Sc}}{(1+\alpha)^{(y-1)}} \sum_y \Big(\sum_{Sc}\Big\{\sum_t\Big[\sum_i \Big(W_{\mathrm{vol}}\left|V_{i,y,Sc,t}^2 - 1\right| : (V_{i,y,Sc,t} \ge V_{\mathrm{thr}}^{\max} \parallel V_{i,y,Sc,t} \le V_{\mathrm{thr}}^{\min}) \\ + \sum_l \left((W_{\mathrm{flow}}\, F_{l,y,Sc,t}^2 : (F_{l,y,Sc,t} \ge F_{\mathrm{thr}})) + W_{loss}(r_l F_{l,y,Sc,t}^2)\right) \\ + W_{EP}(C_{y,Sc,t}^E + \sum_i (CF_i^{\mathrm{DG}} P_{i,y,Sc,t}^{\mathrm{DG}}) + start\_up\ cost) \\ + W_{\mathrm{loss_{DSS}}} \sum_i (\mathrm{loss}_{i,y,Sc,t}^{\mathrm{DSS}}) + W_{\mathrm{Cur}} \sum_i (P_{i,y,Sc,t}^{\mathrm{Cur}})\Big]\Big\}\Big) \end{aligned} \quad (2)$$

$$\sum_i S_i^{\mathrm{DSS}} \le S_{\max}^T \tag{6}$$

$$\sum_i E_i^{\mathrm{DSS}} \le E_{\max}^T. \tag{7}$$

The constraint (3) defines the maximum number of buses, in which DSSs can be installed. The constraints (4) and (5) show the maximum/minimum capacity (power rating and energy) of DSS that can be installed on each particular bus. The constraints (6) and (7) define the maximum of total DSS power rating and energy reservoir capacity that can be installed in the whole network. These two last constraints represent the limitation of the DNOs budget for DSSs installation.

The constraints (8)–(34) are for every scenario (Sc), every time (t) in each day, and every year (y).

2) DSS Operation Constraints:

$$\sum_{t'=0}^{t} ((P_{i,y,Sc,t'}^{\mathrm{DSS}}\Delta t) + loss_{i,y,Sc,t'}^{DSS}) \le E_{i,t'=0}^{\mathrm{DSS}} \tag{8}$$

$$\sum_{t\prime=0}^{t} ((-P_{i,y,Sc,t\prime}^{DSS}\Delta t) - loss_{i,y,Sc,t\prime}^{\mathrm{DSS}}) \le E_i^{\mathrm{DSS}} - E_{i,t\prime=0}^{\mathrm{DSS}} \tag{9}$$

$$-S_i^{\mathrm{DSS}} \le P_{i,y,Sc,t}^{DSS} \le S_i^{\mathrm{DSS}} \tag{10}$$

$$E_{\mathrm{DSS,i}}^{\min} \le E_{i,y,Sc,t}^{\mathrm{DSS}} \le E_i^{\mathrm{DSS}} \tag{11}$$

$$(P_{i,y,Sc,t}^{\mathrm{DSS}})^2 + (Q_{i,y,Sc,t}^{\mathrm{DSS}})^2 \le (S_i^{\mathrm{DSS}})^2 \tag{12}$$

$$loss_{i,y,Sc,t}^{\mathrm{DSS}} = r_i^{\mathrm{DSS}}((P_{i,y,Sc,t}^{\mathrm{DSS}})^2 + (Q_{i,y,Sc,t}^{\mathrm{DSS}})^2) \tag{13}$$

$$P_{i,y,Sc,t}^{\mathrm{DSS}} \le P_{i,y,Sc,t-1}^{\mathrm{DSS}} + RU_i^{\mathrm{DSS}} \tag{14}$$

$$P_{i,y,Sc,t}^{\mathrm{DSS}} \ge P_{i,y,Sc,t-1}^{\mathrm{DSS}} - RD_i^{\mathrm{DSS}}. \tag{15}$$

Equations (8) and (9) refer to the maximum amount of energy that can be stored, or taken, from a generic DSS reservoir. They represent the linking constraints along the hours of a generic day. In particular, (8) means that the sum of all injected and taken energy, including the losses, from the beginning of the day until each generic time interval should be less than initial energy available in the DSS reservoir. Similarly, constraint (9) means that the sum of all injected and taken energy in the DSS reservoir from the beginning of the day to each generic time should be less than the initial available capacity of DSS reservoir. It should be noted that we assumed that the generation/absorption of reactive power from a DSS does not affect its energy-reservoir level. However, like the active power, it increases the DSS losses (e.g., the one taking place into a power electronic converter). Equations (10) and (11) define the maximum and minimum capacity of the DSS reservoir as well as the relevant real-power rating. Equation (12) models the capability curve of a DSS based on the assumption that these devices are interfaced with the grid using a power electronic converter. In this respect, their capability curve is governed by the ampacity limit of the power converter that, in case of an operation under constant ac grid voltage, can be translated into a constraint on the apparent power delivered by the DSS. This nonlinear constraint is linearized into the model by merging an a-priori defined number of linear boundaries approximating the original curve (see Fig. 1). Constraint (13) defines the losses related to DSS active/reactive absorption/production assuming, as a first approximation, the voltage where the DSS is connected is equal to 1 p.u. This constraint is nonconvex, therefore it is relaxed in the problem. The losses related to active and reactive power for each DSS are imposed to be equal or greater than the envelope given by this constraint. Since the losses of the DSSs are also minimized in the objective function, the relaxed inequality constraint is the same as the original equality constraint. Finally, constraints (14) and (15) define the ramp-up and ramp-down limits of the DSS power capability.

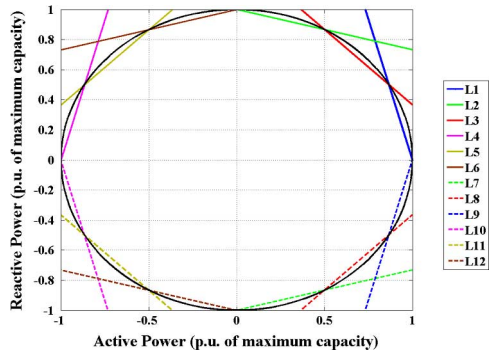

Fig. 1. Linearized DSS capability curve.

3) Network Security Constraints: The SOCP formulation proposed in [25] has been adapted to define the network security constraints together with the representation of the line shunt admittance. This last has been included in terms of a further reactive power generated by the line itself and accounted for the reactive power flow constraint of each line.

Only the square of voltages and current flows appear in the both objective function and constraints. Therefore, the square of voltages and flows are replaced as in

$$v_{i,y,Sc,t} = (V_{i,y,Sc,t})^2 \tag{16}$$

$$f_{ij,y,Sc,t} = (F_{ij,y,Sc,t})^2. \tag{17}$$

The following constraints account, respectively, for the balance of active and reactive power flows on each line feeder:

$$P_{ij,y,Sc,t} = \sum_{k:(j,k)\in C} (P_{jk,y,Sc,t}) + r_{ij} f_{ij,y,Sc,t} + P_{j,y,Sc,t}^{D} - P_{j,y,Sc,t}^{DG} - P_{j,y,Sc,t}^{DSS} - P_{j,y,Sc,t}^{Cur} \tag{18}$$

$$Q_{ij,d,t} = \sum_{k:(j,k)\in C} (Q_{jk,y,Sc,t}) + x_{ij} f_{ij,y,Sc,t} - Q_{ij,y,Sc,t}^{sh} + Q_{j,y,Sc,t}^{D} - Q_{j,y,Sc,t}^{DG} - Q_{j,y,Sc,t}^{DSS} \tag{19}$$

The term C is the set of the lines, which are connected to bus j except the line between buses i and j. Equations (18) and (19) show that the active/reactive flow from bus i to bus j of line between these two buses is equal to the sum of the flows of other lines which are connected to the bus j plus the net injection on the bus j and the losses over the line. The following constraints define the current line flow constraints:

$$f_{ij,y,Sc,t} \ge \frac{(P_{ij,y,Sc,t})^2 + (Q_{ij,y,Sc,t})^2}{v_{i,y,Sc,t}} \tag{20}$$

$$f_{ij,y,Sc,t} \le f_{ij}^{\max} \tag{21}$$

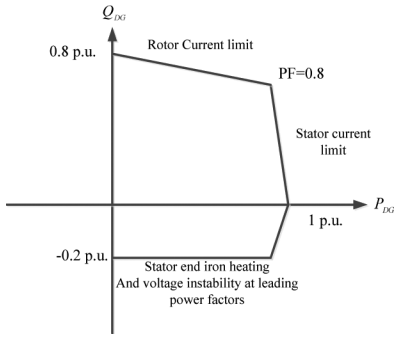

Fig. 2. Linearized DG capability curve.

The constraint (20) is relaxed version of the original one that is equality instead of inequality.

The following equation shows the nodal voltage constraints [25]:

$$v_{j,y,Sc,t} = v_{i,y,Sc,t} - 2(r_{ij}P_{ij,y,Sc,t} + x_{ij}Q_{ij,y,Sc,t}) + (r_{ij}^2 + x_{ij}^2)\left(\frac{(P_{ij,y,Sc,t})^2 + (Q_{ij,y,Sc,t})^2}{v_{i,y,Sc,t}}\right) \quad (22)$$

The quadratic term in (22) is much smaller than the two other terms. Therefore, this term can be neglected. The following constraint has been added to the problem to ensure that the nodal voltages are in the feasible region.

$$v^{\min} \le v_{i,y,Sc,t} \le v^{\max}. \quad (23)$$

Finally, the following constraint accounts for the amount of reactive power related to the shunt impedance of the lines:

$$Q^{\mathrm{sh}}_{j,y,Sc,t} = v_{j,y,Sc,t} b^{\mathrm{sh}}_{j}. \quad (24)$$

4) DGs Constraints:

$$u^{\mathrm{DG}}_{i,y,Sc,t} P^{\min}_{\mathrm{DG_i}} \le P^{\mathrm{DG}}_{i,y,Sc,t} \le u^{\mathrm{DG}}_{i,y,Sc,t} P^{\max}_{\mathrm{DG_i}} \quad (25)$$

$$u^{\mathrm{DG}}_{i,y,Sc,t} Q^{\min}_{\mathrm{DG_i}} \le Q^{\mathrm{DG}}_{i,y,Sc,t} \le u^{\mathrm{DG}}_{\mathrm{DG_i,y,Sc,t}} Q^{\max}_{\mathrm{DG_i}} \quad (26)$$

$$(P^{\mathrm{DG}}_{i,y,Sc,t}, Q^{\mathrm{DG}}_{i,y,Sc,t}) \in \mathrm{DG_i\ Capability\ Curve\ area}. \quad (27)$$

Constraints (25) and (26) define the maximum and minimum active and reactive power that can be produced by dispatchable DGs, respectively. The constraint (27) defines the capability curve of DG generator that is linearized and shown in Fig. 2.

A linear formulation is used for DGs operation and startup costs [29]. The startup cost is modeled by a one step cost function.

Wind turbines and PV panels are assumed to be available in the network as nondispatchable DGs. The output power function formulated in [30] is used here for wind turbines.

D. Linearization of the Objective Function

The voltage deviation minimization and the flow minimization appearing in (2) are not differentiable. However, they are similar to Chebyshev approximation problem and can be replaced by a linear program [31]. Such a linearization process is described in what follows.

Two sets of auxiliary variables are defined for voltage and lines current flows. The obtained linear functions are further constrained as described below. Since only the square of voltage and lines current flows appears in (2), quantities v and f, which are equal to squares of V and F, respectively, are used.

1) Voltage Deviation Minimization:

$$Aux^{V}_{i,y,Sc,t} \ge 0 \quad (28)$$

$$Aux^{V}_{i,y,Sc,t} \ge v_{i,y,Sc,t} - (V^{\max}_{thr})^2 \quad (29)$$

$$Aux^{V}_{i,y,Sc,t} \ge -v_{i,y,Sc,t} + (V^{\min}_{thr})^2. \quad (30)$$

2) Flow Minimization:

$$Aux^{F}_{ij,y,Sc,t} \ge 0 \quad (31)$$

$$Aux^{F}_{ij,y,Sc,t} \ge f_{ij,y,Sc,t} - (F_{thr})^2. \quad (32)$$

The above-mentioned problem is a mixed-integer SOCP (MISOCP) problem with relaxed version of constraints (13) and (20) being the only quadratic terms in the problem. They can be modeled as the second order cone constraints as follows.

$$\left\| \begin{matrix} 2\sqrt{r^{\mathrm{DSS}}_i} P^{\mathrm{DSS}}_{i,y,Sc,t} \\ 2\sqrt{r^{\mathrm{DSS}}_i} Q^{\mathrm{DSS}}_{i,y,Sc,t} \\ 1 - loss^{\mathrm{DSS}}_{i,y,Sc,t} \end{matrix} \right\|_2 \le 1 + loss^{\mathrm{DSS}}_{i,y,Sc,t} \quad (33)$$

$$\left\| \begin{matrix} 2P_{ij,y,Sc,t} \\ 2Q_{ij,y,Sc,t} \\ f_{ij,y,Sc,t} - v_{i,y,Sc,t} \end{matrix} \right\|_2 \le f_{ij,y,Sc,t} + v_{i,y,Sc,t} \quad (34)$$

where (33) and (34) correspond to (13) and (20), respectively.

The YALMIP-MATLAB interface [32] has been selected and used to implement the MISOCP problem, and the GUROBI [33] solver has been used to solve it.

E. Modeling of Scenarios

The input parameters of the optimization problems are characterized by different stochastic behaviors over a given time span. In particular, these variations refer to the following time spans: daily, weekly (including weekdays and weekends especially for the loads), seasonally, and yearly. To deal with these variations, a reasonable number of scenarios should be considered. However, accounting for all possible scenarios results in a large-scale and computationally expensive simulation. Due to this computationally complexity, often the number of scenarios is reduced to a reasonable one characterized by the same degree of volatility/stochasticity of the original scenarios.

In this paper, we used the data clustering method to group the input data and reduce the number of input scenarios. Cluster analysis is used for grouping data according to measured or perceived inherent characteristics or similarity (e.g., [34]). The K-means method is used here to cluster the data since it is one of the most well-known and widely used algorithms for data clustering. As is known, it divides n sets of m-dimensional $\mathbb{R}^m$ data

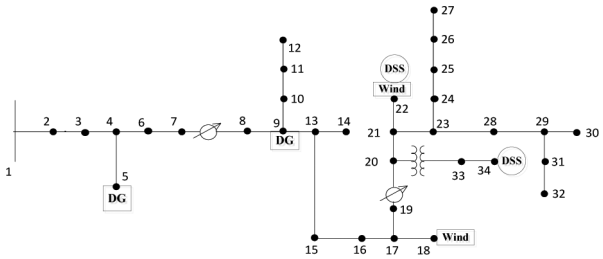

Fig. 3. Modified IEEE 34-bus test feeder. the modifications refer to the presence of the DG units and the grid modeling accounting for the direct sequence parameters only.

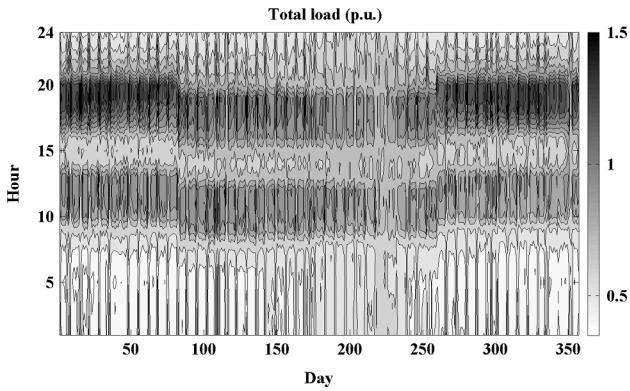

Fig. 4. Initial yearly load profile (base power $S_b = 2.5$ MW).

into k clusters in $\mathbb{R}^m$ and assigns each of the n set to a corresponding k cluster. The method tries to synthesize the k clusters so that the mean square distance from each data of the original set and the synthesized clusters is minimal [34], [35].

A matrix that contains the 24 h of data of the load, PV, wind, and price for all of the days of the year creates the set of used data (in our case, n is equal 365 and m is equal to 96; see Section V for the case study).

III. Simulation and Results

The modified IEEE 34-bus test system [36] is used as a test case (see Fig. 3). It is supposed to have both nondispatchable DGs composed by PV panels and wind turbines and dispatchable DGs. The yearly profile of active power loads for the entire network is shown in Fig. 4. The load profiles are considered to be voltage-independent *PQ* absorptions. Even for PV and wind units, it has also considered that they are voltage-independent active power injections with null reactive power component. Their yearly power production profiles are shown in Figs. 5 and 6. The price scenarios related to the load profiles have been generated by making reference to typical average price of electricity in a region in the southern part of Switzerland and are adjusted by the load profile. The load data corresponds to real measurements recorded into a primary high-to-medium voltage substation. The PV and wind profiles are obtained from [37] and [38], respectively.

The simulation parameters are shown in Table I. It is assumed that PV units are installed on all the load buses and the wind turbines are connected to buses #18 and #22 (see Fig. 3).

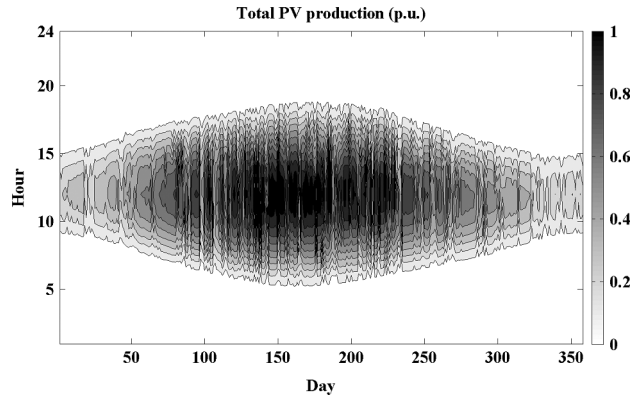

Fig. 5. Initial yearly PV production profile (base power $S_b = 2.5$ MW).

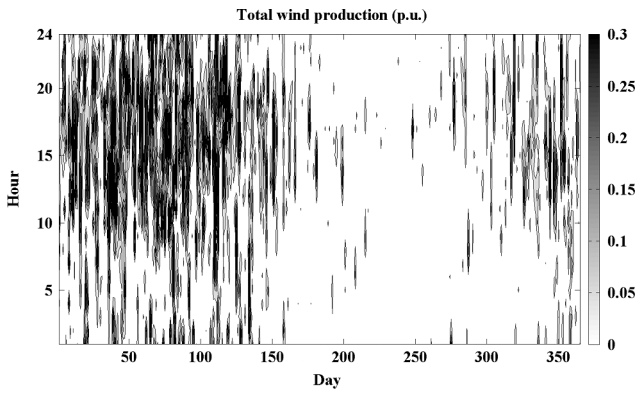

Fig. 6. Initial yearly wind production profile (base power $S_b = 2.5$ MW).

In order to cover the uncertainties and variation of different parameters over the years, we have considered the scenarios of the load, PV, and wind as shown in Figs. 4–6 in addition to price scenarios. As mentioned before, the K-means method is used here to cluster the similar scenarios and reduce their number. A DSS's lifetime of five years has been assumed. The simulation is done for the considered DSS's lifetime, where the parameters' growth/variations are taken into account. The data of each year are grouped into 30 clusters, resulting in 150 scenarios in total. The load growth is considered constant during the lifetime. The wind power capacity is considered to be constant during the lifetime while the PV capacity is considered to have a growth associated with the one of the load since these systems are normally installed on the customers' side. The energy and fuel prices growth over the years are modeled by using the Geometric Brownian Motion (GBM) [39]. Table II shows the pairwise comparison of selected relative weights fed into the AHP.

The scaled coefficients of each term in the objective function, obtained by using the pairwise comparison reported in Table II feeding into AHP, are: $W_{\mathrm{EP}} = 0.0562$, $W_{\mathrm{loss}} = 0.0396$, $W_{\mathrm{vol}} = 0.2535$, $W_{\mathrm{flow}} = 0.6421$, and $W_{\mathrm{lossDSS}} = 0.0086$. The coefficient of load curtailment is considered to be equal to 100. It is equal to the value of the unsupplied load. It should be noted that the coefficient of load curtailment is not considered in the AHP method. In this respect, a large weighting coefficient

TABLE I
SIMULATION PARAMETERS

Base power (energy) value	2.5 MW (MWh)	Maximum number of buses where DSSs can be installed	4
Total PV capacity	1 (p.u.)	Total maximum DSS power rating capacity	0.8 (p.u.)
Total wind capacity	0.3 (p.u.)	Total maximum DSS reservoir capacity	2 (p.u.)
Resistive losses of DSSs	0.04 (p.u.)	DSS ramp-up ramp-down limits	0.3 (MW/h)
Max/min voltage-thresholds beyond which voltage deviation is minimized	+/- 3%	Max feeder current-threshold beyond which current feeder flow is minimized	80 %
Start-up cost of DGs	2 ($)	Operation cost of DGs parameters	(1 $/h, 17 ($/MWh))
Annual load growth	2%	Interest rate	3%
Average energy price from external grid in first year	36 ($/MWh)	GBM sigma	0.08
Capital investment cost of DSSs	5000 ($)	Installation cost of DSSs power rating	1200 ($/kW) [39]
Installation cost of DSSs energy reservoir	4000 ($/kWh) [39]	Maintenance cost of DSSs	100 ($/MWh/year)
Dispatchable DGs total maximum capacity	0.2 (p.u.) (2 units)		

TABLE II
PAIRWISE COMPARISIONS OF THE OBJECTIVE TERMS

	Voltage deviation	Total network losses	Energy cost from external grid	Total Feeders overloading	DSSs losses
Voltage deviation	1	5	7	1/4	12
Total Network losses	1/5	1	1/2	1/8	5
Energy cost from external grid	1/7	2	1	1/9	8
Total Feeders over-loading	4	8	9	1	15
DSSs losses	1/12	1/5	1/8	1/15	1

has been considered in order to prevent at most the load curtailment. The coefficient adopted to weight the cost of energy consumed from the external grid has been chosen to weight the installation and maintenance costs of DSSs ($\mathrm{Obj}_{\mathrm{inv}}$). This decision is based on the need of having an homogeneity that is required by the elements of the objective function quantifying the cost elements for both investments and operation.

Table III shows the optimal obtained DSS locations and relevant sizes. From the results of Table III, we can see that two buses are selected by the proposed method to host the DSSs.

In order to quantify the benefits associated with the optimal DSS placement, in what follows we have reported the results of two cases corresponding to: case 1 with optimal allocated DSSs

TABLE III
OBTAINED OPTIMAL DSS LOCATION AND SIZE (BASE POWER $S_B = 2.5$ MW)

bus	22	34
DSS power rating (p.u.)	0.33	0.39
DSS reservoir capacity (p.u.)	0.88	1.05

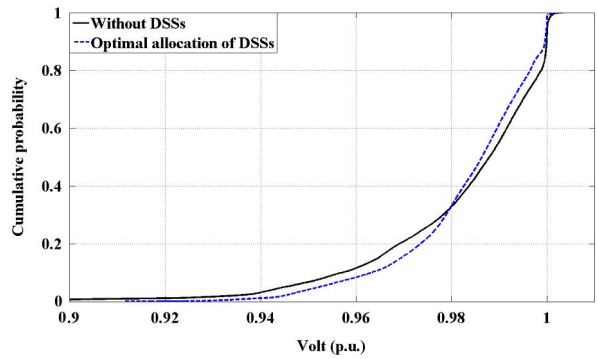

Fig. 7. Node voltage CDFs for the case with and without optimally planned DSSs.

TABLE IV
CHANGES IN EACH TERM OF THE OBJECTIVE FUNCTION ALONG FIVE YEARS (BASE POWER/ENERGY IS EQUAL 2.5 MW/MWH)

	Total network energy losses (p.u)	Total energy cost ($)	Total feeders loading with percentages larger than 80% (p.u.)	Total load curtailment (p.u.)
Optimal DSS allocation	742.89	2151700	0	0
Without DSS	770.33	2609000	206.4393	691.91

and case 2 without DSS. In particular, the cumulative distribution functions (CDFs) of the voltages related to both cases 1 and 2 associated with the whole time period and for all of the network buses are shown in Fig. 7. These results show that the optimal solution improves the voltage profiles with reference to the case without DSS. In particular, it can be observed that the presence of voltages below 0.94 p.u. and larger than 1 p.u. is decreased essentially to zero. Further, the voltages exhibit a larger probability in correspondence of an interval closer to the desired voltage.

Changes of the other terms of the objective function during the lifetime (i.e., total losses, energy cost, feeders loading, and load curtailment) are shown in Table IV. These results show that all the elements of the objective function, exhibit significant improvements. In addition to the total losses reduction, the total cost of supplied energy, which includes the energy imported from the external grid as well as the energy supplied by local DG units, is significantly reduced.

Furthermore, the presence of load curtailment and feeders overloading (representing the first and second goals in the objective function) are entirely eliminated with the proposed optimal placement of DSSs. These two terms correspond to the potential network upgrades required without the presence of DSSs.

The daily operation cycle of the two DSSs provided by the case 1 in correspondence of two days (one day in winter and one

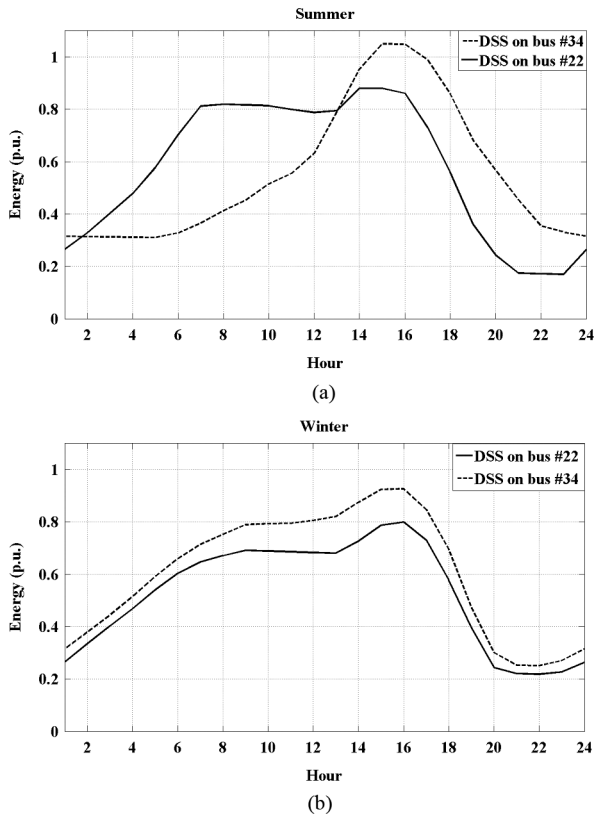

Fig. 8. Profiles of the energy reservoir levels of the two DSSs during (a) one summer day and (b) one winter day (base energy $Eb = 2.5$ MWh.

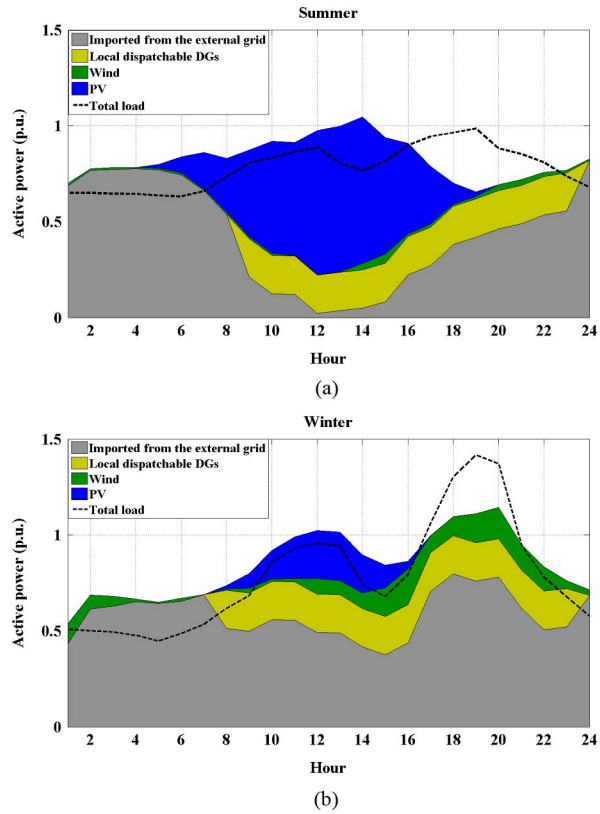

Fig. 9. Active power profiles of load, PV, wind, and two dispatchable DGs during (a) one summer day and (b) one winter day (base power $Sb = 2.5$ MW).

day in summer of the first year) are shown in Fig. 8. In particular, Fig. 8(a) shows the p.u. energy stored in the two DSS units for the summer day and Fig. 8(b) the winter day. From these two figures, it can be observed that, since the available PV production in summer days is much higher compared with winter ones, DSSs tend to use their available reservoir to achieve the optimality of the objective function. Furthermore, in summer days, the DSSs are used to store the power produced by the renewable resources in the mid-hours of the day (essentially the energy produced by PVs) and supply it back to the grid during high peak hours. As can also be seen from these results, the satisfaction of the daily storage SoC is fulfilled.

The total active load, PV, wind, and dispatchable DGs power productions are shown in Fig. 9. In particular, Fig. 9(a) is related to a generic summer day and Fig. 9(b) to a generic winter day. It can be observed that, in the winter days, the DSS are used to accumulate energy in the first two-third of the day (from both the external grid and, when available, wind and PV supply), in order to support the grid in the peak hours in which high prices appears. Concerning the case of summer days, it can be seen that the DSS accumulate energy in the central part of the day (essentially from PV) in order to behave similarly to winter days in the peak hours. It should be underlined that these objectives are always reached by supporting the quality of the supply (i.e., voltage control, feeders congestion, and losses minimization).

IV. Conclusion

The paper has proposed a MISOCP formulation of a problem aiming at optimally allocating DSSs into ADNs. The capability of DSSs to support the network in terms of: 1) network voltage deviations; 2) feeders congestion; 3) network losses; 4) cost of supplying loads (from external grid or local producers); and 5) load curtailment has been accounted to find their best locations and sizes. Furthermore, the problem is able to account for the investment costs related to the DSS installation and maintenance.

The proposed approach is also characterized by a convexification of the targeted problem enabling its fast/accurate solution. This peculiarity has allowed the analysis of multiple scenarios, generated by a suitable data clustering method. It accounts for the stochastic behavior of both loads and renewables together with their evolution in terms of growth and price changes along the DSS lifetime.

The IEEE 34-bus test feeder, suitably modified to account for the presence of dispatchable and nondispatchable distributed generation, has been used to demonstrate the effectiveness and capability of the proposed method. A five-year time-span has been assumed to perform the optimal analysis. The obtained results have shown the capability of the proposed method to optimally allocate DSSs to: 1) largely improve the quality of supply of the ADN in terms of mitigating voltage deviations, eliminating line congestions and load curtailment and 2) minimizing the total cost of locally-used electricity and investment cost for DSSs installation and maintenance.

It is possible to conclude that optimally allocated DSSs can represent a valid solution for ADN operators that do not want to deploy massive DG controls. This opportunity will potentially postpone large control infrastructure deployment as well as grid infrastructure reinforcement.

REFERENCES

[1] N. Jenkins, R. Allan, P. Crossley, D. Kirschen, and G. Stcbac, *Embedded Generation*. London, U.K.: Inst. Elect. Eng, 2000.

[2] J. A. P. Lopes, N. Hatziargyriou, J. Mutalc, P. Djapic, and N. Jenkins, "Integrating distributed generation into electric power systems: A review of drivers, challenges and opportunities," *Elect. Power Syst. Res.*, vol. 77, no. 9, pp. 1189–1203, Jul. 2007.

[3] M. E. Elkhatib, R. El-Shatshat, and M. M. A. Salama, "Novel coordinated voltage control for smart distribution networks with DG," *IEEE Trans. Smart Grid*, vol. 2, no. 4, pp. 598–605, Dec. 2011.

[4] M. Nick, M. Hohmman, R. Cherkaoui, and M. Paolone, "On the optimal placement of distributed storage systems for voltage control in active distribution networks," in *Proc. IEEE Int. Conf. Smart Grids Technol.*, Europe, 2012, pp. 1–6.

[5] P. M. S. Carvalho, P. F. Correia, and L. A. F. Ferreira, "Distributed reactive power generation control for voltage rise mitigation in distribution networks," *IEEE Trans. Power Syst.*, vol. 23, no. 2, pp. 766–772, May 2008.

[6] T. Sels, C. Dragu, T. V. Craenenbroeck, and R. Belmans, "Overview of new energy storage systems for an improved power quality and load managing on distribution level," in *Proc. 16th Int. Conf. and Exhibition on Electricity Distribution, Part 1: Contributions*, 2001, pp. 1–5.

[7] A. Oudalov, R. Cherkaoui, and A. Beguin, "Sizing and optimal operation of battery energy storage system for peak shaving application," in *Proc. IEEE Lausanne Powertech*, Lausanne, Switzerland, 2007, pp. 621–625.

[8] J. P. Barton and D. G. Infield, "Energy storage and its use with intermittent renewable energy," *IEEE Trans. Energy Conv.*, vol. 19, no. 2, pp. 441–448, Jun. 2004.

[9] M. Zillmann, Y. Ruifeng, and T. K. Saha, "Regulation of distribution network voltage using dispersed battery storage systems: A case study of a rural network," in *Proc. IEEE PES Gen. Meeting*, 2011, pp. 1–8.

[10] P. Mercier, R. Cherkaoui, and A. Oudalov, "Optimizing a battery energy storage system for frequency control application in an isolated power system," *IEEE Trans. Power Syst.*, vol. 24, no. 3, pp. 1469–1477, Aug. 2009.

[11] Y. M. Atwa and E. F. El-Saadany, "Analytical approaches for optimal placement of distributed generation sources in power systems," *IEEE Trans. Power Syst.*, vol. 19, no. 4, pp. 2068–2076, Nov. 2004.

[12] D. Gautam and N. Mithulananthan, "Optimal DG placement in deregulated electricity market," *Electr. Power Syst. Res.*, vol. 77, no. 12, pp. 1627–1636, Oct. 2007.

[13] G. Celli, E. Ghiani, S. Mocci, and F. Pilo, "A multi-objective evolutionary algorithm for the sizing and siting of distributed generation," *IEEE Trans. Power Syst.*, vol. 20, no. 2, pp. 750–757, May 2005.

[14] Z. Liu, F. Wen, and G. Ledwich, "Optimal siting and sizing of distributed generators in distribution systems considering uncertainties," *IEEE Trans. Power Del.*, vol. 26, no. 4, pp. 2541–2551, Oct. 2011.

[15] C. Chen, S. Duan, T. Cai, B. Liu, and G. Hu, "Optimal allocation and economic analysis of energy storage system in microgrids," *IEEE Trans. Power Electron.*, vol. 26, no. 10, pp. 2662–2773, Oct. 2011.

[16] Y. M. A. E. F. El-Saadany, "Optimal allocation of ESS in distribution systems with a high penetration of wind energy," *IEEE Trans. Power Syst.*, vol. 25, no. 4, pp. 1815–1822, Nov. 2010.

[17] G. Carpinelli, F. Mottola, D. Proto, and A. Russo, "Optimal allocation of dispersed generators, capacitors and distributed energy storage systems in distribution networks," *Modern Electr. Power Syst.*, pp. 1–6, 2010.

[18] G. Celli, S. Mocci, F. Pilo, and M. Loddo, "Optimal integration of energy storage in distribution networks," *IEEE PowerTech*, pp. 1–7, 2009.

[19] Y. Makarov, P. Du, M. Kintner-Meyer, C. Jin, and H. Illian, "Sizing energy storage to accommodate high penetration of variable energy resources," *IEEE Trans. Sustain. Energy*, vol. 3, no. 1, pp. 34–40, Jan. 2012.

[20] K. Christakou, J.-Y. Le Boudec, M. Paolone, and D.-C. Tomozei, "Efficient computation of sensitivity coefficients of node voltages and line currents in unbalanced radial electrical distribution networks," *IEEE Trans. Smart Grids*, vol. 4, no. 2, pp. 741–750, Jun. 2013.

[21] M. Nick, M. Hohmman, R. Cherkaoui, and M. Paolone, "Optimal location and sizing of distributed storage systems in active distribution networks," in *Proc. IEEE PowerTech*, 2013, pp. 1–6.

[22] J. Lavaei and S. H. Low, "Zero duality gap in optimal power flow problem," *IEEE Trans. Power Syst.*, vol. 27, no. 1, pp. 92–107, Feb. 2012.

[23] M. Farivar, C. R. Clarkey, S. H. Low, and K. M. Chandy, "Inverter VAR control for distribution systems with renewables," in *Proc. Int. Conf. Smart Grid Commun.*, 2011, pp. 457–462.

[24] L. Gan, N. Li, U. Topcu, and S. Low, "On the exactness of convex relaxation for optimal power flow in tree networks," in *Proc. IEEE Annu. Conf. Decision and Control*, 2012, pp. 465–471.

[25] O. A. Taylor and F. S. Hover, "Convex models of distribution system reconfiguration," *IEEE Trans. Power Syst.*, vol. 27, no. 3, pp. 1407–1413, Aug. 2012.

[26] M. Lobo, L. Vandenberghe, S. Boyd, and H. Lebret, "Applications of second-order cone programming," *Linear Algebra and its Applicat.*, vol. 284, no. 1, pp. 193–228, Nov. 1998.

[27] F. Alizadeh and D. Goldfarb, "Second-order cone programming," *Math. Program.*, vol. 95, no. 1, pp. 3–51, Jan. 2003.

[28] T. L. Saaty, "Decision making—The analytic hierarchy and network processes (AHP/Anp)," *J. Syst. Sci. Syst. Eng.*, vol. 13, no. 1, pp. 1–35, Mar. 2004.

[29] M. Carrión and J. M. Arroyo, "A computationally efficient mixed-integer linear formulation for the thermal unit commitment problem," *IEEE Trans, Power Syst.*, vol. 21, no. 3, pp. 1371–1378, Aug. 2006.

[30] M. Zhao, Z. Chen, and F. Blaabjerg, "Probabilistic capacity of a grid connected wind farm based on optimization method," *Renewable Energy*, vol. 31, no. 13, pp. 2171–2187, Oct. 2006.

[31] S. Boyd and L. Vandenberghe, *Convex Optimization*. Cambridge, U.K: Cambridge Univ., 2004.

[32] J. Löfberg, "YALMIP: A toolbox for modeling and optimization in MATLAB," in *Proc. CACSD Conf.*, Taipei, Taiwan, 2004, pp. 284–289.

[33] *"Gurobi Optimizer Reference Manual,"* Gurobi Optimization, Inc. , 2012 [Online]. Available: http://www.gurobi.com

[34] A. K. Jain, "Data clustering: 50 years beyond K-means," *Pattern Recognit. Lett.*, vol. 31, no. 8, pp. 651–666, Jan. 2010.

[35] T. Kanungo, D. M. Mount, N. S. Netanyahu, C. D. Piatko, R. Silverman, and A. Y. Wu, "An efficient k-means clustering algorithm: Analysis and implementation," *IEEE Trans Pattern Anal. Mach. Intell.*, vol. 24, no. 7, pp. 881–892, Jul. 2002.

[36] "IEEE Distribution Planning Working Group, Radial distribution test feeders," *IEEE Trans. Power Syst.*, vol. 6, pp. 975–985, Aug. 1991.

[37] "Solar Irradiation Data (SODA)." [Online]. Available: http://www.soda-is.com/eng/index.html

[38] "Homer Energy." [Online]. Available: http://homerenergy.com/

[39] M. T. Barlow, "A diffusion model for electricity prices," *Math. Finance*, vol. 12, no. 4, pp. 287–298, Oct. 2002.

[40] D. Rastler, "Electricity energy storage technology options: a white paper primer on applications, costs and benefits," *Electr. Power Res. Inst.*, pp. 23–25, Dec. 2010.

Mostafa Nick (S'12) was born in Iran in 1986. He received the M.S. degree in electrical engineering from Amirkabir University of Technology (Tehran Polytechnic), Tehran, Iran, in 2011. He is currently working toward the Ph.D. degree at the Distributed Electrical System Laboratory, École Polytechnique Fédérale de Lausanne (EPFL), Lausanne, Switzerland.

His current research interests include planning problems of active distribution networks, distributed energy storage modeling and relevant applications for real-time operation of electrical distribution grids.

Rachid Cherkaoui (SM'10) received the M.S. degree in electrical engineering and Ph.D. degree from École Polytechnique Fédérale de Lausanne (EPFL), Lausanne, Switzerland, in 1983 and 1992, respectively. His doctoral work was in the field of optimal operation topologies for distribution systems.

From 1983 to 1987, he was with Entreprises Electriques Fribourgeoises (Swiss electrical utility) developing a state estimator and security analysis tools for the HV transmission system of that company. From 1987 to 1992, he joined the Power System Laboratory, École Polytechnique Fédérale de Lausanne (EPFL), Lausanne, Switzerland. From 1993 to 2009, he was leading the research activities in the field of optimization and simulation techniques applied to electrical power and distribution systems. Since 2009, as senior scientist, he is the head of the power system group (PWRS) at EPFL. Presently, the main research topics of his group are concentrated on electricity market deregulation, distributed generation and storage with reference to distribution systems and smart grids, and power system vulnerability mitigation. He is the author or coauthor of more than 100 scientific publications.

Dr. Cherkaoui is a member of technical program committees of various conferences. He was member of CIGRE task forces C5–2 (2003–2006) and working group C5–7 (2006–2011) related to electricity market deregulation, and IEEE Swiss Chapter officer (2005 –2011). He serves regularly as reviewer for different journals and conferences. He was the recipient of the ABB Swiss Award'93.

Mario Paolone (SM'10) was born in Italy in 1973. He received the M.Sc. degree (with honors) in electrical engineering and Ph.D. degree from the University of Bologna, Bologna, Italy, in 1998 and 2002, respectively.

In 2005, he was appointed Researcher in Electric Power Systems, University of Bologna, Bologna, Italy, where he was with the Power Systems Laboratory until 2011. In 2010, he became an Associate Professor with the Politecnico di Milano, Milan, Italy. Currently, he is an Associate Professor with the École Polytechnique Fédérale de Lausanne, Lausanne, Switzerland, where he accepted the EOS Holding Chair of Distributed Electrical Systems Laboratory. He is author or coauthor of over 170 scientific papers published in reviewed journals and presented at international conferences. His research interests are in power systems with particular reference to real-time monitoring and operation, power system protections, power systems dynamics, and power system transients.

Prof. Paolone is secretary and member of several IEEE and Cigré Working Groups. He was co-chairperson of the Technical Committee of the 9th edition of the International Conference of Power Systems Transients (IPST 2009). In 2013, he was the recipient of the IEEE EMC Society Technical Achievement Award.